Electronic Supplementary Material (ESI) for RSC Advances.

Supplementary Information

Folding and Structural Polymorphism of G-quadruplex Formed from a Long Telomeric Sequence Containing Six GGG tracts

Atsushi Tanaka, Jungkweon Choi,[a] and Tetsuro Majima**

The Institute of Scientific and Industrial Research (SANKEN), Osaka University, Mihogaoka 8-1, Ibaraki, Osaka 567-0047, Japan.

[a] Present address: Center for Nanomaterials and Chemical Reactions, Institute for Basic Science (IBS), Daejeon 305-701, Republic of Korea.

Experimental Section

Determination of Thermodynamic Parameters: In order to correct melting curves regarding lower and higher baselines, we used the equation below:

$$A_{295nm} = \frac{\left((a+bx) + (c+dx)\exp\left(\frac{\Delta H}{R}\left(\frac{1}{T} - \frac{1}{T_m} \right) \right) \right)}{1+\exp\left(\frac{\Delta H}{R}\left(\frac{1}{T} - \frac{1}{T_m} \right) \right)} \qquad \text{(S1)}$$

where $A_{295\,nm}$ is the normalized absorbance observed at 295 nm; $a + bx$ and $c + dx$ are the linear functions of the two baselines; ΔH, R, T and T_m are the enthalpy, gas constant, temperature and melting temperature, respectively.

The Gibbs free energy (ΔG) and entropy (ΔS) and at 25℃ were calculated by

$$\Delta G_{298K} = T\Delta H\left(\frac{1}{T} - \frac{1}{T_m} \right) \qquad \text{(S2)}$$

$$\Delta S = \frac{\Delta H - \Delta G}{T} \qquad \text{(S3)}$$

The acquired thermodynamic parameters are summarized in Table S1.

Fluorescence correlation spectroscopy (FCS): FCS experiments carried out with a time-resolved fluorescence microscope using confocal optics (MicroTime 200; PicoQuant, Berlin-Adlershof, Germany). We used 2 nM sample solutions for measuring FCS curves with various concentrations of K^+ ions. In order to measure the molecular diffusion time, 60 μL of DNA solution was loaded into the micro-chamber made by a 1-inch glass cover slip and Secure-Seal (S24733, Invitrogen). The FAM of samples were excited through an oil objective (Olympus, UAPON 150XOTIRF; 1.45 NA, 150x) with a 485 nm pulsed laser (PicoQuant, full width at half-maximum 120 ps) controlled by a PDL-800B driver (PicoQuant). The excitation power of 33 μW was used and photons were collected into 1 ms bins for 1 hour. The fluorescence was collected with the same objective and detected by a single photon avalanche photodiode (Micro Photon Devices, PDM 50CT and 100CT) through a dichroic beam splitter, bandpass filter (Olympus, D680/40M), and 75 μm pinhole for spatial filtering to reject out-of-focus signals. The data collected using the PicoHarp 300 TCSPC module (PicoQuant) were stored in the time-tagged time-resolved mode (TTTR), recording every detected photon with its individual timing, which were used for the single-molecule analysis. In FCS, the autocorrelation function of the fluorescence intensity, $G(\tau)$, is given by

$$G(\tau) = \frac{\langle I(t) \cdot I(t+\tau) \rangle}{\langle I(t) \rangle^2} \qquad \text{(S4)}$$

where $I(t)$ is the fluorescence intensity at time t, $I(t+\tau)$ is the fluorescence intensity after a time lag τ, and $\langle\rangle$ denotes the time average over the total observation time.

Table S1. $K^+_{1/2}$ and *n* values for G-quadruplex-forming sequences determined by E_{FRET} and CD intensities (I_{CD}).

Sequences	**Monitored parameter**	***n***	$\mathbf{K^+_{1/2}}$
25htel	E_{FRET}	1.8 ± 0.1	10.1 ± 0.4
37htel		0.7 ± 0.1	117.0 ± 21.7
I-1/2		0.7 ± 0.1	132.3 ± 26.2
I-1/6		1.0 ± 0.1	239.3 ± 49.4
I-4/5		1.1 ± 0.1	77.5 ± 5.1
I-4/6		1.1 ± 0.1	154.4 ± 15.3
I-5/6		0.7 ± 0.1	271.6 ± 57.5
37htel	I_{CD}	1.5 ± 0.1	14.1 ± 1.1
I-1/2		1.8 ± 0.1	10.3 ± 0.3
I-1/6		1.9 ± 0.1	22.9 ± 1.2
I-4/5		3.3 ± 0.1	62.7 ± 0.9
I-4/6		3.1 ± 0.1	60.3 ± 2.3
I-5/6		1.6 ± 0.1	18.0± 1.0

Table S2. Melting temperatures (T_m) and thermodynamic parameters of G-quadruplex-forming sequences determined at various [K^+].

Sequences	[K^+] (mM)	T_m (K)	$-\Delta G_{298K}$ (kcal mol^{-1})	ΔH (kcal mol^{-1})	ΔS (cal $K^{-1}\cdot mol^{-1}$)
37htel	60	315	1.98 ± 0.01	36.7 ± 0.2	117 ± 1
	120	323	3.08 ± 0.01	39.8 ± 0.2	123 ± 1
	170	332	3.64 ± 0.02	35.6 ± 0.2	107 ± 1
	320	341	5.20 ± 0.02	41.2 ± 0.2	121 ± 1
	520	345	6.93 ± 0.27	50.0 ± 2.0	144 ± 6
I-1/2	60	318	2.71 ± 0.04	43.9 ± 0.5	138 ± 2
	120	325	3.54 ± 0.03	42.8 ± 0.4	132 ± 1
	170	329	4.09 ± 0.05	42.9 ± 0.5	130 ± 2
	320	338	4.35 ± 0.06	36.4 ± 0.6	107 ± 2
	520	347	4.73 ± 0.07	33.4 ± 0.7	96 ± 2
I-1/6	60	308	1.24 ± 0.01	38.2 ± 0.2	124 ± 1
	120	319	2.11 ± 0.02	32.0 ± 0.2	100 ± 1
	170	324	2.75 ± 0.02	34.3 ± 0.2	106 ± 1
	320	333	3.43 ± 0.04	32.7 ± 0.3	98 ± 1
	520	341	3.87 ± 0.04	30.7 ± 0.3	90 ± 1
I-4/5	60	303	0.54 ± 0.01	32.5 ± 0.2	107 ± 1
	120	310	1.40 ± 0.01	36.2 ± 0.2	117 ± 1
	170	316	2.03 ± 0.02	35.6 ± 0.3	113 ± 1
	320	326	3.12 ± 0.02	36.4 ± 0.2	112 ± 1
	520	333	3.56 ± 0.04	33.7 ± 0.4	101 ± 1
I-4/6	60	300	0.29 ± 0.01	44.0 ± 0.5	147 ± 2
	120	308	1.42 ± 0.01	43.8 ± 0.2	142 ± 1
	170	313	1.89 ± 0.01	39.4 ± 0.2	126 ± 1
	320	325	2.78 ± 0.01	33.4 ± 0.2	103 ± 1
	520	333	3.59 ± 0.01	34.1 ± 0.1	102 ± 1
I-5/6	60	311	1.78 ± 0.01	42.5 ± 0.3	137 ± 1
	120	321	2.87 ± 0.02	40.0 ± 0.3	125 ± 1
	170	326	3.43 ± 0.03	40.0 ± 0.4	123 ± 1
	320	334	3.98 ± 0.04	37.0 ± 0.4	111 ± 1
	520	341	4.58 ± 0.05	36.3 ± 0.4	106 ± 1

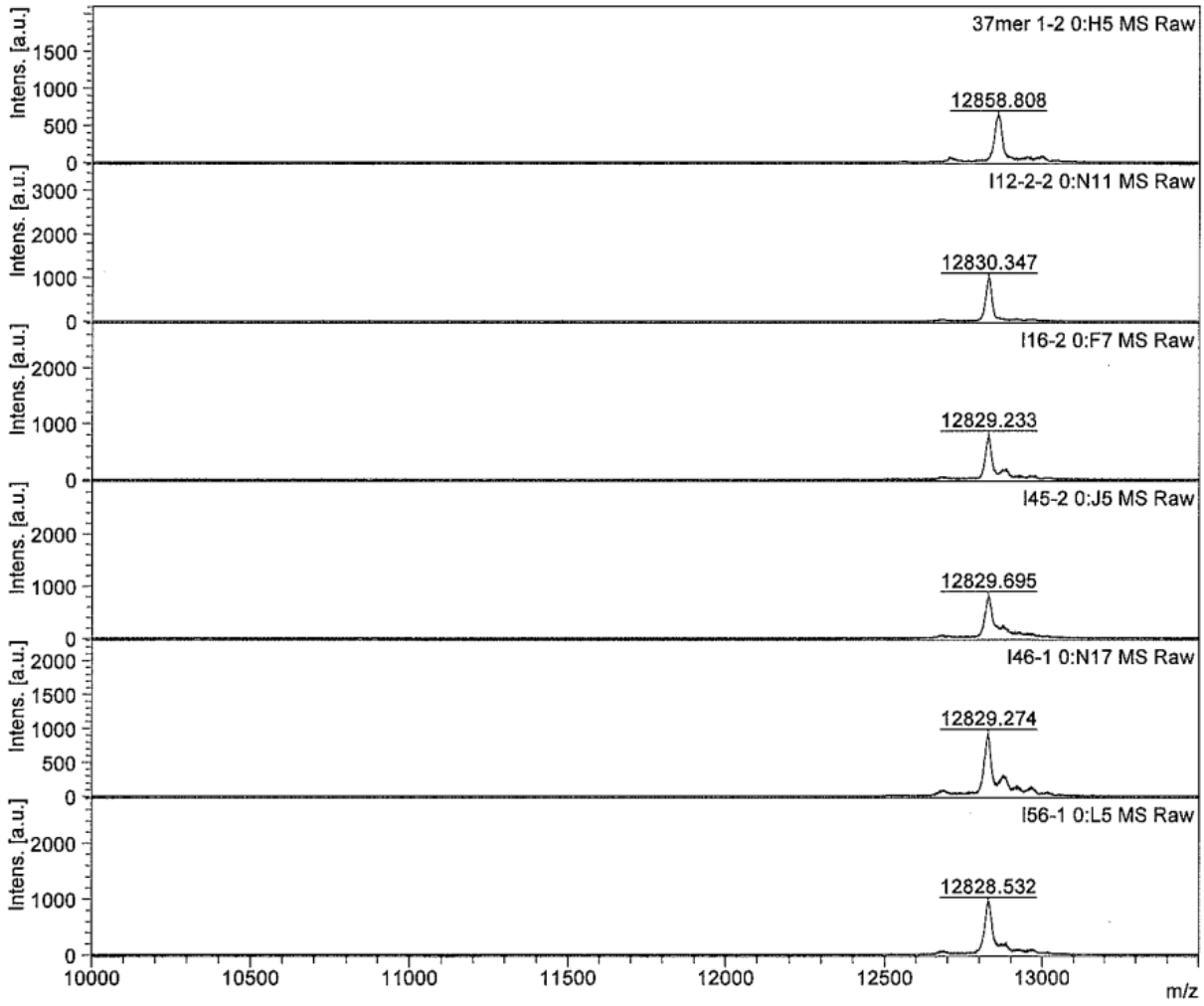

Figure S1. Mass spectra of *37htel*, I-1/2, I-1/6, I-4/5, I-4/6 and I-5/6 (from top to bottom).

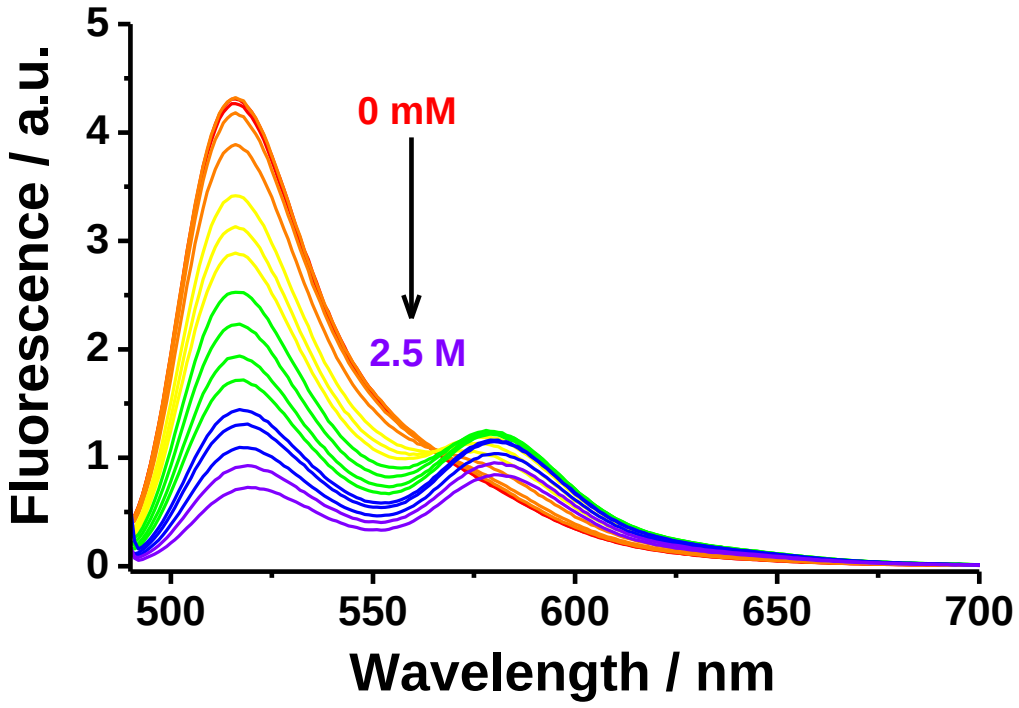

Figure S2. Changes in the fluorescence spectrum of *37htel* as a function of [K^+]. ([*37htel*] = 168 nM; [K^+] = 0 mM (red) ~ 2.5 M (purple)).

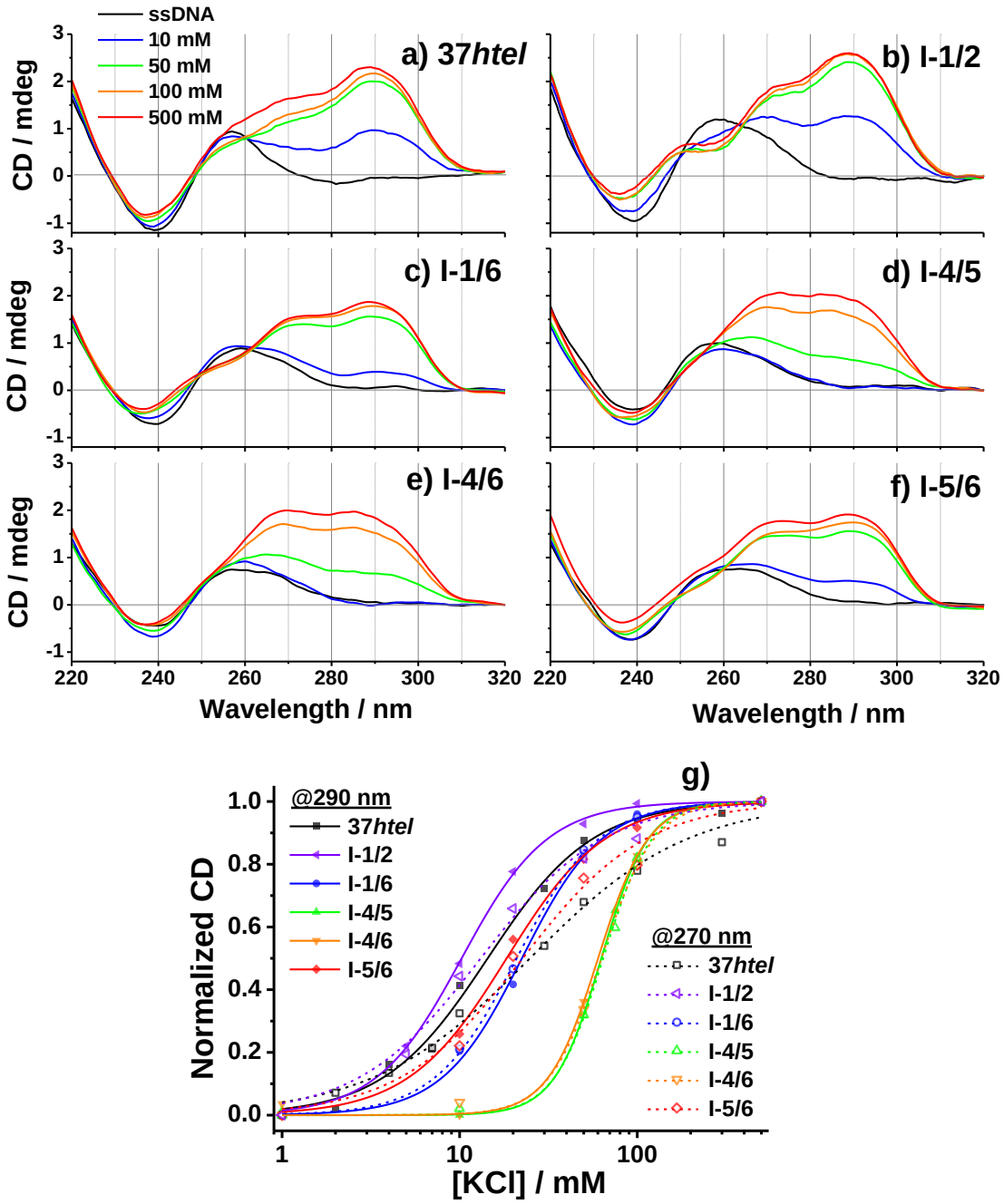

Figure S3. a-f) CD spectra of *37htel*, I-1/2, I-1/6, I-4/5, I-4/6, and I-5/6 with various [K^+]. ([DNA] = 10 μM). g) Changes in I_{CD} for *37htel*, I-1/2, I-1/6, I-4/5, I-4/6, and I-5/6 as a function of [K^+]. Theoretical curves obtained from the fitting analysis are shown in straight lines.

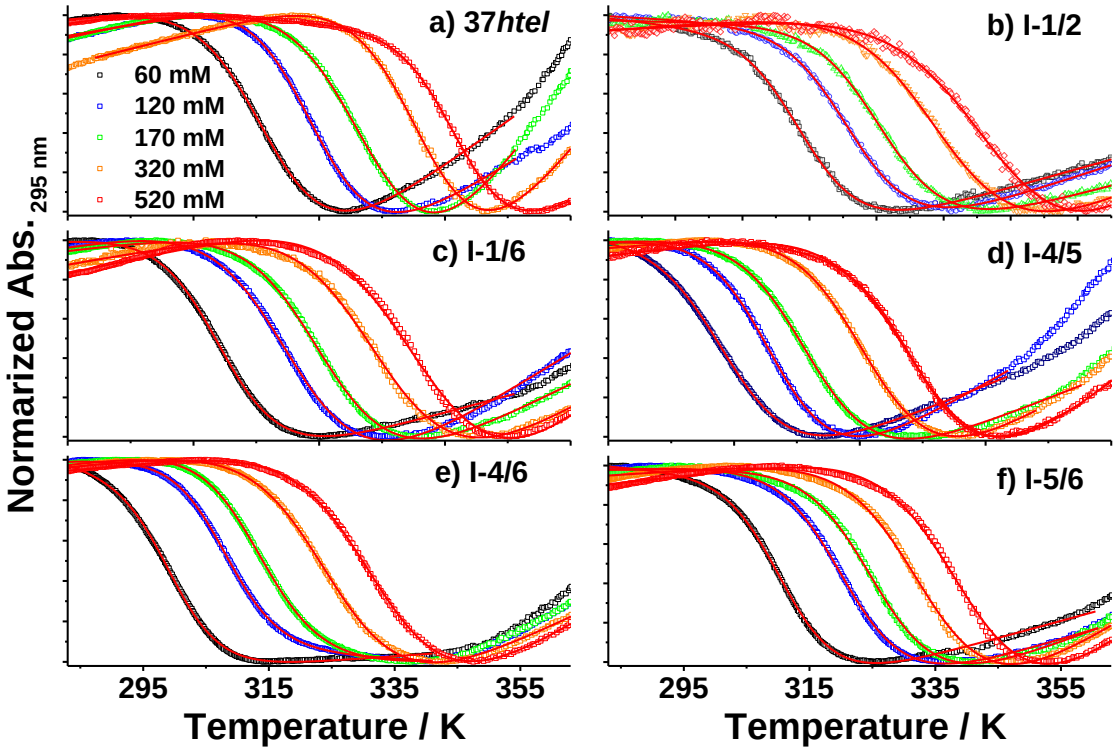

Figure S4. Thermal denaturation curves monitored at 295 nm measured for *37htel*, I-1/2, I-1/6, I-4/5, I-4/6, and I-5/6 with various [K^+]. ([DNA] = 5 μM). Theoretical fit obtained from the fitting analysis is shown in red.